Preservation of Serotonin-Mediated Contractility in Adult Sheep Pulmonary Arteries Following Long-Term High-Altitude Hypoxia

Demosthenes G. Papamatheakis,[1] Srilakshmi Vemulakonda,[1] Quintin Blood,[4] Ravi Goyal,[4]
Monica Rubalcava,[5] Kurt Vrancken,[2,4] Allison Bennett,[6] Antoinette Dawson,[6] Noah J. Osman,[6]
Arlin B. Blood,[2,4] William J. Pearce,[3,4] Lawrence D. Longo,[3,4] and Sean M. Wilson[1,3–5]

Abstract

Papamatheakis, Demostehens G., SrilakshmiVemulakonda, Quintin Blood, Ravi Goyal, Monica Rubalcava, Kurt Vrancken, Allison Bennett, Antoinette Dawson, Noah J. Osman, Arlin B. Blood, William J. Pearce, Lawrence D. Longo, and Sean M. Wilson. Preservation of serotonin-mediated contractility in adult sheep pulmonary arteries following long-term high-altitude hypoxia. *High Alt. Med. Biol.* 12:253–264.—Long-term hypoxia (LTH) can increase serotonin (5-HT) signaling as well as extracellular calcium entry in adult rodent pulmonary arteries (PA), and 5-HT is associated with pulmonary hypertension. Because LTH, 5-HT, and calcium entry are related, we tested the hypothesis that LTH increases 5-HT-mediated PA contractility and associated calcium influx through L-type Ca^{2+} channels, nonselective cation channels (NSCC), and reverse-mode sodium-Ca^{2+} exchange. We performed wire myography and confocal calcium imaging on pulmonary arteries from adult ewes that lived near sea level or were maintained at high-altitude (3801 m) for $\sim$110 days. LTH did not increase the arterial medial wall thickness, nor did it affect the potency or efficacy for 5-HT-induced PA contraction. Ketanserin (100 nM), a 5-HT_{2A} antagonist, shifted the 5-HT potency to a far greater extent than 1 μM GR-55562, a 5-$HT_{1B/D}$ inhibitor. These influences were unaffected by LTH. The rank order for reducing 5-HT-induced PA contraction in normoxic animals was extracellular calcium removal $\approx$ 10 mM Ni^{2+} $\approx$ 10 μM verapamil $\approx$ 10 μM nifedipine with 50 μM SKF 96365 > 30 μM KB-R7943 $\approx$ 100 μM flufenamic acid $\approx$ 10 μM nifedipine $\approx$ 100 μM Gd3 + > 100 μM La^{3+} > 500 μM Ni^{2+} $\approx$ 10 μM diltiazem $\approx$ 50 μM 2-APB $\approx$ 100 μM LOE 908. Contraction was not reduced by 100 μM spermine or 30 μM SN-6. LTH increased the effects of KB-R7943 and mitigated those of nifedipine but did not affect calcium responses in imaging studies. Overall, in adult sheep, arterial structure and 5-HT_{2A} and 5$HT_{1B/D}$ functions are preserved following LTH while the role of NSCC-related calcium-dependent contraction is increased. These elements indicate preservation of PA contractility in LTH with minimal functional changes.

Introduction

LONG-TERM HYPOXIA (LTH), such as occurs at high-altitude, can lead to a number of problems including pulmonary hypertension. The development of pulmonary hypertension due to long-term hypoxia is multifactorial, with various neurohumoral factors released from the endothelium, platelets, neuroepithelial and mast cells being important to this process. Several of the major factors, include serotonin (5-hydroxytryptamine; 5-HT), platelet derived growth factor, platelet activating factor, endothelin-1 (ET-1), prostaglandins, and vascular endothelial growth factor (Bixby et al., 2007; Toga et al., 1992; Voelkel and Tuder, 1995). Among these, 5-HT is one of the most potent vasoconstrictors of the pulmonary vasculature (Heffner et al., 1987; Wilson et al., 2005). Moreover, multiple studies have confirmed that hypoxia due to high altitude or other LTH environments can cause 5-HT release (Lauweryns et al., 1983). Related to this, LTH increases 5-HT-mediated pulmonary vascular reactivity in rats (Keegan et al., 2001; MacLean et al., 1996; MacLean et al., 2000). 5-HT-mediated pulmonary arterial vasoconstriction occurs largely due to the activation of 5-HT_2 receptors

[1]Division of Pulmonary and Critical Care, Department of Medicine and [2]Division of Neonatology, Department of Pediatrics, Loma Linda University Medical Center, Loma Linda, California.
[3]Department of Physiology and Pharmacology, [4]Center for Perinatal Biology, and [5]Advanced Imaging and Microscopy Core, Loma Linda University, Loma Linda, California.
[6]University of Mississippi Light Microscopy Core, Department of Pharmacology School of Pharmacy, University of Mississippi, Oxford, Mississippi.

(Wilson et al., 2005) that in turn activate Gq-coupled pathways, which increases cytosolic calcium (Ca^{2+}) and stimulates arterial contraction. The rise in cytosolic Ca^{2+} is dependent upon both Ca^{2+} release from the sarcoplasmic reticulum and extracellular Ca^{2+} entry (Wilson et al., 2005). Ca^{2+}-permeable ion channels and transport pathways contribute to the extracellular Ca^{2+} entry and associated pulmonary arterial vasoreactivity (Lin et al., 2004; Shimoda et al., 2000; Wilson et al., 2005; Yang et al., 2006).

LTH alters the function of Ca^{2+}-permeable ion channels in pulmonary arterial smooth muscle. In rats, LTH decreases the role of L-type Ca^{2+} channels (Ca_L) during ET-1 stimulation (Shimoda et al., 2000). By comparison, nonselective cation channel (NSCC) activity is augmented by LTH in rat pulmonary arterial myocytes (Lin et al., 2004) and in human pulmonary arterial myocytes from patients with pulmonary hypertension (Yu et al., 2004). Therefore, LTH results in many changes in Ca^{2+}-dependent signaling and contractility in the pulmonary vasculature with a substantial effect on extracellular Ca^{2+} influx. Nonetheless, the changes that may occur in 5-HT-mediated Ca^{2+}-dependent vascular reactivity with LTH, and its mechanistic underpinnings, are unknown. The effect of LTH on cardiovascular function is influenced greatly by the species examined. Sheep, dogs, and guinea pigs are thought to be hyporesponsive with regards to the development of pulmonary hypertension and vascular reactivity. Rats, rabbits, and humans have moderate responses to LTH, while cattle and pigs have the most marked responses (Penaloza and Arias-Stella, 2007; Tucker et al., 1975). To advance the understanding of the effects of LTH on pulmonary vascular function, we examined the influence of high-altitude acclimatization on adult sheep. The general premise is that, by comparing LTH acclimatization to LTH to the adjustments of more severe responders, beneficial adaptations can be distinguished from markers important to the pathogenesis of pulmonary hypertension. These comparisons also will help to discriminate epiphenomenon from causal factors. In these experiments, we assessed whether LTH in adult sheep alters serotonergic-mediated contraction and the role of extracellular Ca^{2+} entry in a manner similar to that previously documented for the rat. Specifically, we tested the hypothesis that high-altitude acclimatization decreases the role of Ca_L, and increases that of NSCC Ca^{2+} entry pathways, during 5-HT$_{2A}$-mediated pulmonary arterial contractility.

Methods

Experimental animals

All experimental procedures were performed within the regulations of the Animal Welfare Act, the National Institutes of Health Guide for the Care and Use of Laboratory Animals, "The Guiding Principles in the Care and Use of Animals" approved by the Council of the American Physiological Society, and the Animal Care and Use Committee of the University of Mississippi and Loma Linda University (LLU). We conducted these studies on 4th and 5th order pulmonary arteries with internal diameters of about 500–700 μm, from adult ewes that lived at Nebeker Ranch (Lancaster, CA; 720 m) and were brought to LLU (353 m; arterial $P_{AO2} = 95 \pm 5$ Torr) for experimental study or were acclimatized to high-altitude (3801 m, $P_{AO2} = 60 \pm 5$ Torr) at the Barcroft Laboratory, White Mountain Research Station (Bishop, CA) for ∼110 days (Longo et al., 1996). Animals maintained at high altitude were

transported to LLU and shortly after arrival, a tracheal catheter was placed in the ewe, through which N_2 flowed at a rate adjusted to maintain P_{AO2} at ∼60 Torr (Kamitomo et al., 1994), which is equivalent to the oxygen tension at the White Mountain Research Station. This P_{AO2} was maintained until the time of the experimental study. Within 1 to 5 days after arriving at LLU, sheep were sacrificed with an overdose of the proprietary euthanasia solution, Euthasol (pentobarbital sodium 100 mg/Kg and phenytoin sodium 10 mg/Kg; Virbac, Ft. Worth, TX). Lungs were removed and transported on ice (4°–5°C) to the University of Mississippi via overnight express, or used immediately for contractility experiments at LLU. To avoid complications from endothelium-mediated effects, the endothelium was removed by carefully inserting a small roughened hypodermic needle or rotating the artery on the mounting wire (Wilson et al., 2005). Endothelium removal was confirmed by contracting vessels with 125 mM KCl (high-K) and at the plateau adding 10 μM acetylcholine. A lack of a vasodilatory response indicated that the endothelium was disrupted appropriately.

Tissue preparation

Pulmonary arteries for contractility and live-cell confocal microscopy studies were dissected free of parenchyma and cut into 5 mm long rings in ice-cold phosphate-free balanced salt solution (BSS) of the following composition (mM): 126 NaCl, 5 KCl, 10 HEPES, 1 MgCl$_2$, 2 CaCl$_2$, and 10 glucose; pH 7.4 (adjusted with NaOH). This BSS was used for live-cell confocal imaging studies and contraction experiments that were performed with inorganic inhibitors, including Ni^{2+}, Gd^{3+}, and La^{3+}. All other contraction studies were performed with a modified Krebs-Henseleit (K-H) solution containing (mM): 120 NaCl, 4.8 KCl, 1.2 K$_2$HPO$_4$, 25 NaHCO$_3$, 1.2 MgCl$_2$, 2.5 CaCl$_2$, and 10 glucose.

Contraction studies

Contraction studies were performed using wire myography techniques. Wire myography has been used extensively and has been instrumental in evaluating the importance of multiple pathways that determine vascular smooth muscle tone in pulmonary and systemic arteries (Hirenallur et al., 2008; Longo et al., 1996; Ng et al., 2007; Shimoda et al., 2000; Wilson et al., 2005). Myography studies such as these are widely performed because they allow the experimenter to focus on specific aspects of vascular smooth muscle contraction in ways that cannot be performed *in vivo*.

Myography experiments were performed on pulmonary arterial rings suspended in organ baths (Radnoti Glass Instruments, Inc. Monrovia, CA) that contained 5 or 10 ml of modified K-H solution maintained at 37°C and aerated with 95% O_2–5% CO_2 (pH = 7.4) or unaerated BSS. Arterial rings treated with high concentrations of Ni^{2+}, as well as Gd^{3+}, La^{3+}, or low concentration of Ni^{2+} were bathed in nonaerated phosphate-free BSS to prevent chelation (Ng et al., 2007). Each ring was suspended between two tungsten wires passed through the lumen. One wire was anchored to the glass hook at the bottom of the organ chamber; the other connected to a tissue hook attached to a low compliance force transducer (Radnoti Glass Instruments Inc.) for the measurement of isometric force (Wilson et al., 2005). The transducers were connected to an analogue-to-digital data interface (Digidata 1200, Molecular Devices, Sunnyvale, CA; MIO-16, National

Instruments, Austin, TX; Powerlab 16/30 A/D Instruments, Colorado Springs, CO; or MP100, Biopac, Goleta, CA) attached to a computer. The changes in tension were recorded using pClamp 8.1 software (Molecular Devices) at the University of Mississippi, or Labview 3.1 (National Instruments), Chart 5.5 (AD Instruments, Colorado Springs, CO), or Acq Knowledge 3.9 (Biopac, Systems, Inc.) at Loma Linda University, and the obtained data were stored on magnetic or optical media for later analysis. At the beginning of each experiment, vessels were equilibrated without tension for 30 min to 1 h. Vessel rings were tensioned to 444 ± 44 dynes in 265 vessels from 20 normoxic sheep and 482 ± 16 dynes in 231 vessels from 17 LTH sheep ($p = 0.17$) by stretching the vessels progressively, as previously described (Wilson et al., 2005). Isolated pulmonary arterial rings were stimulated with 125 mM KCl, which causes membrane depolarization and subsequent Ca_L activation.

This procedure allows for comparative evaluation of 5-HT-induced smooth muscle contraction and CaL activation. Moreover, published evidence indicates that long-term hypoxia may enhance pulmonary vascular reactivity and reduce Ca_L function in rat (Shimoda et al., 2000) or increase Ca_L function in newborn pig (Hirenallur et al., 2008). In many experiments, the tension was normalized for comparison to the maximum response obtained with 10 μM 5-HT (%T5-HTmax). In other experiments, the tension was normalized to the maximum response obtained with high-K (%TKmax). Lumen diameter was calculated based on visual measurements of arterial perimeter, made with a stage micrometer at the end of the experiment using a stereo microscope (Nikon SMZ-1, Melville, NY). For evaluating dose-response characteristics, arteries were stimulated by applying cumulatively 1 nM to 100 μM 5-HT in log increments without washing in-between each 5-HT concentration increase.

Confocal microscopy studies

The cytosolic calcium was measured in pulmonary arterial myocytes *in-situ,* with the Ca^{2+}-sensitive dye Fluo-4 AM (Invitrogen, Carlsbad, CA) using a Zeiss 510 META laser scanning confocal imaging workstation (Thornwood, NY) with an inverted microscope (Zeiss Axiovert 200). Fluo-4 AM was dissolved in DMSO and added from a 10 mM stock to the arterial suspension at a final concentration of 10 μM, along with 0.1% pluronic F127 for 1–1.5 h at room temperature in the dark in BSS. Arterial segments were then washed for 30 min to allow for dye esterification, and cut into linear strips. The arterial segments were pinned to Sylgard blocks (Ellsworth Adhesives, Germantown, WI), placed in an open bath imaging chamber (Warner Instruments, Hamden, CT), and mounted on the confocal imaging stage. In some cases, the arteries were perfused at $\sim$1 ml/min using a peristaltic pump (Rainin, Oakland, CA) with an electronic pinch valve system (Automate Scientific, Berkeley, CA), while in others, the arteries were maintained in a static bath. Cells were illuminated at 488 nm with a krypton argon laser and the emitted light was collected using a photomultiplier tube for frames of 512 X 512 pixels with a long pass filter > 505 nm. Images were acquired using bi-directional scanning techniques, where the photomultiplier tube recorded the light intensity while the galvanometer driven mirror moved in both directions. This effectively doubled the acquisition rate, where full frame images were generated every 700–900 msec. To ensure that

we were able to collect images from as many arterial myocytes as possible, the pinhole was adjusted to provide an imaging depth of $\sim$10 μm. Based on morphological examination of fixed and live preparations, this depth is approximately the width of two cells (data not shown). Generally, images were acquired at a 12-bit sampling depth, but occasionally an 8-bit depth was used. Most recordings were made using a water immersion 40X c-Apochromat (numerical aperture, NA 1.2) objective, but a 20X non-immersion (NA 0.8) or 63X oil immersion Plan Apochromat (NA 1.4) also were used. The acquisition depth and objective used did not influence the spatial-temporal characteristics presented in this study. Regions of interest were examined *post-hoc*, and analyzed using Zeiss LSM image examiner. For presentation purposes the fractional fluorescence intensity was calculated:

$$F/Fo = F\text{-baseline}/Fo\text{-baseline}$$

where baseline is the intensity from a region of interest with no cells, F is the fluorescence intensity for the region of interest, and Fo is the fluorescence intensity during a period from the beginning of the recording when there was no Ca^{2+} activity.

In separate studies, the numbers of nuclei were recorded to estimate the percentage of arterial myocytes with Ca^{2+} oscillations and to measure the thickness of the arterial wall. These recordings were made in parallel arteries from the same groups of animals. To estimate the percentage of myocytes with Ca^{2+} oscillations, the tissue was labeled with Cy3-conjugated anti-α-smooth muscle actin (Sigma-Aldrich), and sealed with Vectashield mounting medium containing DAPI (H-1200, Vector Labs, Burlingame, CA). Images were recorded serially through the whole arterial wall; from the luminal side through the adventitial layers at $\sim$ 0.3 μm increments 1024 X 1024, 12 bit using a 63X oil immersion Plan Apochromat (NA 1.4) objective. A pinhole size corresponding to an imaging depth of $\sim$0.6 μm was used, which resulted in overlapping images through the z-axis. Once mounted, preparations were imaged by exciting Cy3 with a 543 nm and DAPI with a 405 nm laser on a Zeiss 510 META confocal microscope. For Cy3, emitted light was collected with a confocal PMT with a long pass filter > 560 and for DAPI light was collected through a band-pass filter of 420–480 nm. We chose the regions staining positive for Cy3 and DAPI for morphological evaluation, and measured the numbers of cell nuclei per 1000 μm^2. The number of cells ranged between 10 and 13 per 1000 μm^2, and there were no significant differences between vessels obtained from normoxic and LTH sheep. The thickness of the arterial wall was measured in a separate series of experiments where arteries were labeled with anti-α-smooth muscle actin and alexa fluor 555 to visualize the smooth muscle layer and Hoescht to visualize nuclei. Non-specific binding of Hoescht to the adventitia and lamina was used to measure total wall thickness. Setting the confocal pinhole to the optimal imaging depth, we optically measured the thickness of the arterial wall and the smooth muscle layer in multiple locations for each sample.

The Ca^{2+} oscillation recordings were made in pulmonary arterial myocytes of three animals from each group. In normoxic animals, 18 control regions of interest (ROI) were examined in control conditions and 24 ROI examined in the presence of 10 μM 5-HT while in LTH sheep 15 ROI were examined in both control and 5-HT conditions. Moreover, in normoxic sheep 60 myocytes were examined in control

conditions and 87 in the presence of 5-HT while in hypoxic sheep 13 myocytes were examined under control conditions and 40 were examined in the presence of 5-HT.

Chemicals and drugs

Most reagents and chemicals were purchased from Sigma-Aldrich. Fluo-4 AM and Pluronic F127 were purchased from Invitrogen (Carlsbad, CA), KBR and SN-6 from Tocris (Ellisville, MO), and SKF from Tocris or Sigma-Aldrich.

Statistical methods

All time-series recordings were graphed with IGOR pro 6.0 (Wavemetrics, Lake Oswego, OR), and the data presented as mean±S.E.M. Statistical analyses were made using GraphPad Prism 5.0 (La Jolla, CA). Data was evaluated for normality prior to any comparative statistical analysis. Between groups that were distributed normally, statistical difference was determined with a 2-tailed unpaired Student's t-test. A Mann-Whitney U test was used for comparisons of non-normal data. For confocal studies, comparisons were made within and among groups using a two-way ANOVA and Bonferroni post-hoc analyses. Dose-response curves were fitted in Prism 5.0 using a Hill equation (Wilson et al., 2005). The n/N values reported reflect the total number of arterial segments and total number of sheep tested respectively. $P < 0.05$ was accepted as statistically significant.

Results

A previous study indicates that sheep acclimatize to long-term high altitude living while other models develop pulmonary dysfunction (Tucker et al., 1975). With regards to the pulmonary vasculature, there can be thickening of the smooth muscle layer, which is thought to contribute to the generation of pulmonary hypertension. Functional and structural studies were performed on pulmonary arteries isolated from adult sheep to provide a more comprehensive view of potential changes associated with the acclimatization response to high altitude living. Stimulation of arterial segments with high-K allows for comparative evaluation of 5-HT-induced arterial contraction and for Ca_L importance (Ward and Snetkov, 2004). The average force for K^+-dependent contraction in arteries isolated from normoxic (1273 ± 153 dynes; $N = 15$) sheep was the same as the force generated in arteries from LTH (1680 ± 262 dynes; $N = 12$) sheep ($p = 0.17$). In our study, the average force of $10 \mu M$ 5-HT-induced pulmonary artery contraction also did not differ between normoxic (2303 ± 201 dynes; $N = 20$) and LTH (1976 ± 189 dynes; $N = 11$) sheep ($p = 0.29$). Thus, LTH did not alter the fundamental contraction due to either direct membrane depolarization or to neurohumoral stimulation with serotonin.

To assess changes in $5-HT_{2A}$ and $5-HT_{1B/D}$ receptor subtypes due to LTH, we applied cumulative doses of 5-HT to pulmonary arterial segments from normoxic and LTH animals, in the presence or absence of selective antagonists for $5-HT_{2A}$ receptors ($100 nM$ Ketanserin) and $5-HT_{1B/D}$ receptors ($1 \mu M$ GR-55562–GR). The peak contractility responses at each dose were recorded, normalized to the high-K^+ response, plotted, and then fit with a simple logistic binding equation. Figure 1 shows the resulting dose response curves of normalized pulmonary artery contractility against the logarithm of 5-HT concentrations. There were no statistically significant
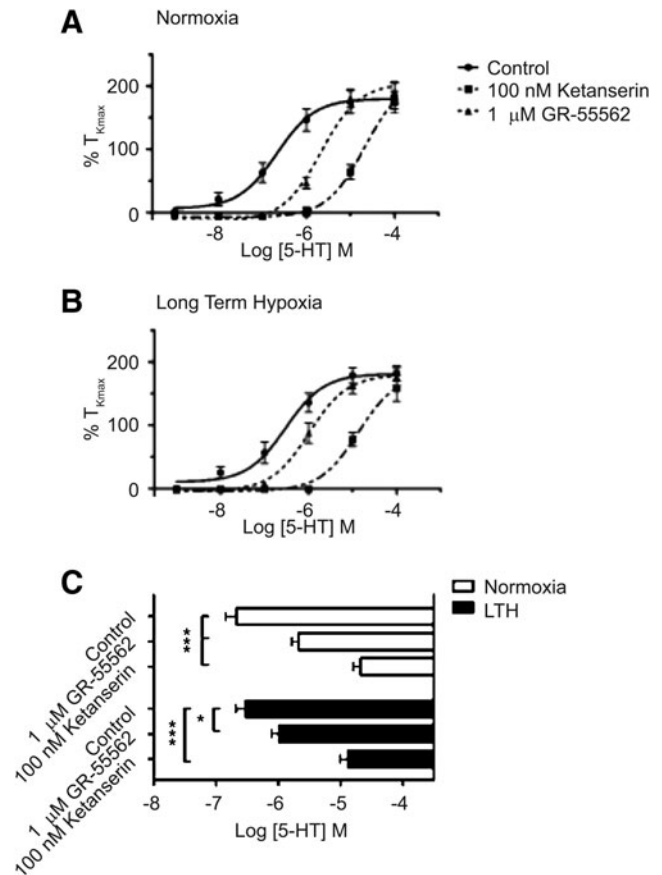

FIG. 1. Ketanserin and GR-55562 inhibit 5-HT-mediated pulmonary arterial contractility. Dose response curves of pulmonary arterial rings exposed to $1 nM$ to $100 \mu M$ of 5-HT in an additive manner from **(A)** normoxic and **(B)** LTH sheep. *Solid lines* indicate absence of any antagonists (Control). *Dotted lines* indicate presence of $100 nM$ ketanserin (*boxes*) or $1 \mu M$ GR-55562 (*triangles*). Curves are plotted in relation to the maximal contraction induced by initial stimulation of $125 mM$ K+K-H solution (%TKmax). **(C)** *Bars* (*open:* normoxic; *solid:* LTH) indicate mean±S.E.M. of EC50 values for each dose response curve depicted in **(A)** and **(B)**. *$p < 0.05$, ***$p < 0.001$ denotes significant difference by 2-way ANOVA.

differences in the maximal contraction regardless of the presence or absence of antagonists both intra- and inter-LTH and normoxic groups ($p > 0.05$). In normoxic sheep, we noted a statistically significant right shift of the $logEC_{50}$ in the presence of GR (-5.67 ± 0.11; $n = 12/N = 3$) or Ketanserin (-4.68 ± 0.12; $n = 14/N = 3$) compared to control (-6.67 ± 0.18; $n = 13/N = 4$). Similar results were noted in LTH sheep with the presence of GR (-5.99 ± 0.12; $n = 10/N = 3$) or Ketanserin (-4.88 ± 0.13; $n = 9/N = 3$) compared to controls (-6.52 ± 0.16; $n = 9/N = 3$). These results indicate that the roles of $5-HT_{1B/D}$ and $5HT_{2A}$ receptors are unaffected by LTH stress. Moreover, the relative potency of these antagonists indicates that $5-HT_{2A}$ receptors, which are commonly coupled with Gq proteins and linked to contractility via Ca^{2+}-dependent signaling pathways, are of greater importance than $5-HT_{1B/D}$ receptors, which are coupled through G_i mechanisms (Hinton et al., 2000).

To examine the extent to which LTH alters the role of extracellular Ca^{2+} entry with 5-HT-elicited pulmonary arterial

contraction, we performed studies in the presence and absence of extracellular Ca^{2+}. Figures 2A and 2B show representative recordings from individual pulmonary arteries from these experiments. As expected, extracellular Ca^{2+} removal severely restricted 5-HT-mediated pulmonary artery contraction. The average contractile responses, shown as a percentile relative to an initial 10 μM 5-HT stimulated response,
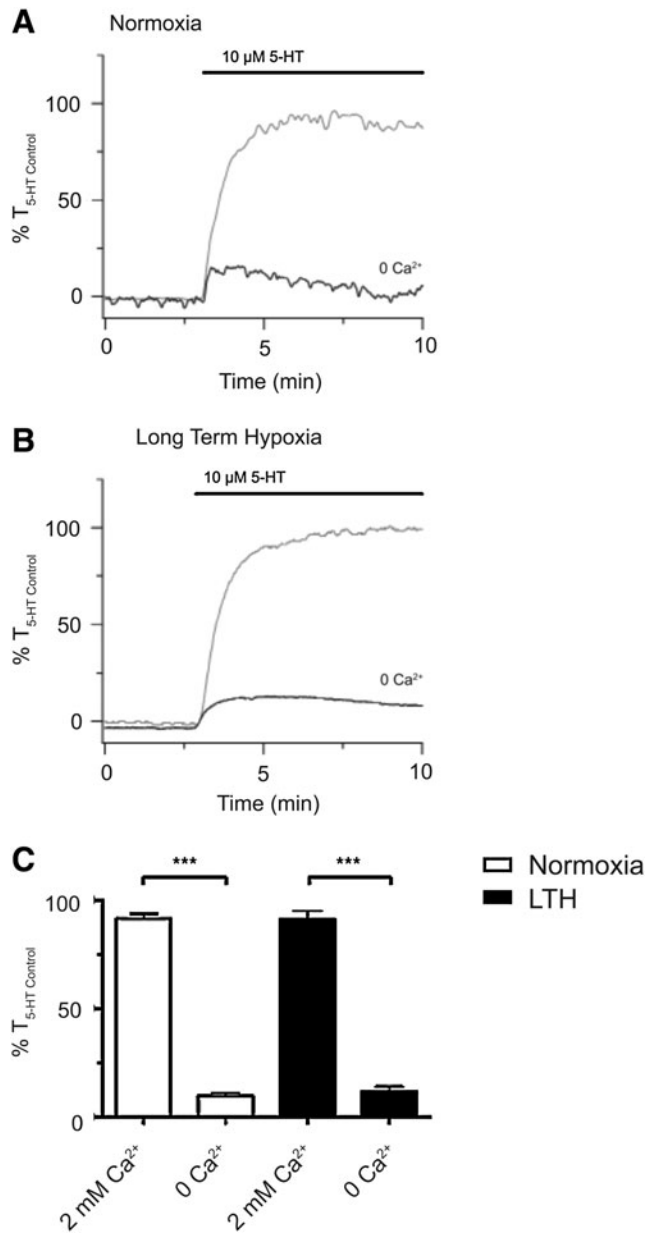
are illustrated in Figure 2C. In arteries from normoxic sheep, there were significant differences between control vessels ($92 \pm 2\%$; $n=14/N=4$), and vessels without extracellular $Ca2+$($10 \pm 2\%$; $n=15/N=4$). Similar results were noted in LTH sheep (91 ± 4 %, $n=17/N=5$ vs. $12 \pm 2\%$, $n=20/N=5$ respectively).

The importance of extracellular Ca^{2+} to pulmonary arterial contractility was confirmed by repeating the above experiments in the presence and absence of 10 mM nickel (Ni^{2+}). In comparison to removal of extracellular Ca^{2+}, high concentrations of Ni^{2+} potently inhibit Ca^{2+} influx through Ca_L (Hollywood et al., 2003), NSCC (Wilson et al., 2005), and reverse mode Na^+–Ca^{2+} exchange (Hobai et al., 1997). The response to 10 mM Ni^{2+} was similar in both LTH and normoxic conditions, and comparable to the results from the zero-Ca^{2+} experiment shown in Figure 2. Figure 3 summarizes the change in contraction of the pulmonary arteries as a percentile of an initial 10 μM 5-HT control dose, both in the presence and absence of 10 mM Ni^{2+} in vessels from normoxic ($10 \pm 2\%$; $n=13/N=3$ vs. $84 \pm 6\%$; $n=12/N=3$) and LTH sheep ($28 \pm 6\%$; $n=13/N=4$ vs. $98 \pm 6\%$; $n=16/N=4$). These results support the proposition that extracellular Ca^{2+} entry is vital to pulmonary artery contraction regardless of their acclimatization to LTH.

To assess the extent to which LTH limits the role of Ca_L in 5-HT-mediated pulmonary arterial contraction, we stimulated arteries in the presence and absence of three major classes of Ca_L blockers. These include dihydropyridines (10 μM nifedipine), benzothiazepines (10 μM diltiazem), and phenylalkylamines (10 μM verapamil). Figure 4E shows that the average pulmonary arterial contraction responses to 10 μM 5-HT were similar in the presence of: 0.1% DMSO in normoxic ($97 \pm 5\%$; $n=21/N=7$) and LTH ($105 \pm 7\%$, $n=23/N=8$) animals; 10 μM diltiazem in normoxic ($75 \pm 8\%$; $n=10/N=4$) and LTH ($84 \pm 5\%$; $n=13/N=4$) animals; and 10 μM verapamil in normoxic ($16 \pm 5\%$; $n=9/N=4$) and LTH ($7 \pm 3\%$; $n=13/N=4$) animals. Nevertheless, 10 μM nifedipine reduced contraction to a greater extent in vessels from normoxic ($56 \pm 5\%$, $n=14/$

FIG. 2. Extracellular Ca^{2+} is vital for 5-HT-elicited pulmonary arterial contractility. Isometric tension recording of pulmonary arterial rings constricted in the presence (*gray tracing*) or absence (*black tracing*) of 2 mM extracellular Ca^{2+} from **(A)** normoxic and **(B)** LTH sheep. Tracings are plotted in relation to maximal contraction from an initial 10 μM 5-HT stimulation (% T5-HT Control). **(C)** *Bars* indicate mean ± S.E.M. of 5-HT-induced contraction expressed as % T5-HT Control in the presence or absence of extracellular Ca^{2+} for pulmonary arteries from normoxic (*open*) and LTH (*solid*) adult sheep. ***$p < 0.001$) denotes significant difference by 2-way ANOVA.
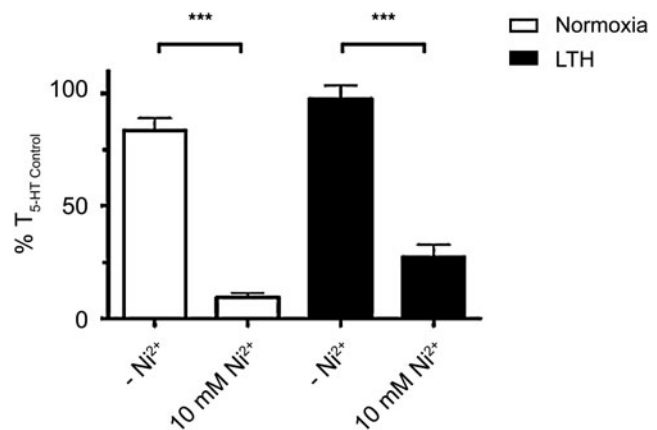

FIG. 3. Ni^{2+} blocks 5-HT-mediated pulmonary arterial contractility. *Bars* indicate mean ± S.E.M. based on isometric tension recordings of pulmonary arterial rings constricted with 10 μM 5-HT in the presence of 10 mM Ni^{2+} or absence of Ni^{2+} from normoxic (*open*) and LTH (*solid*) adult sheep. Values of 5-HT-induced contraction are expressed as % T5-HT Control in the absence or presence of 10 mM Ni^{2+}. ***$p < 0.001$) denotes significant difference by 2-way ANOVA.
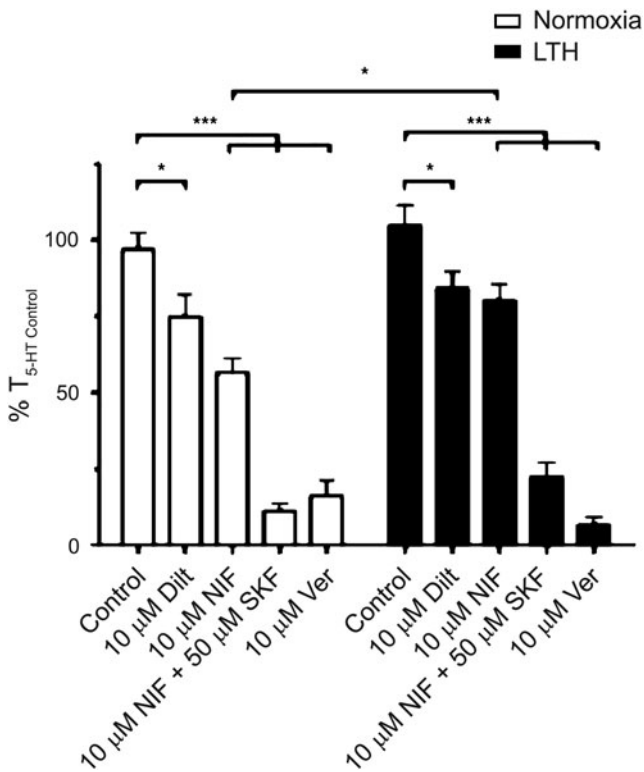
FIG. 4. The role for L-type Ca^{2+} channels during 5-HT-mediated pulmonary arterial contractility may be affected by LTH in sheep. *Bars* indicate mean ± S.E.M. based on isometric tension recordings of pulmonary arterial rings constricted with 10 μM 5-HT in the presence of 0.1% DMSO, 10 μM nifedipine (NIF), 10 μM nifedipine plus 50 μM SKF 96365, 10 μM diltiazem (Dilt), or 10 μM Verapamil (Ver) from normoxic (*open*) and LTH (*solid*) sheep. Values of the 5-HT induced contraction are expressed as % T5-HT Control in the presence or absence of the above antagonists. *$p < 0.05$, ***$p < 0.001$ denotes significant difference by 2-way ANOVA.

$N = 5$) as compared to LTH (80 ± 6%, $n = 20/N = 8$) sheep. The findings that nifedipine and diltiazem account for only a portion of the Ca^{2+}-dependent contraction, while verapamil, extracellular Ca^{2+} removal and 10 mM Ni^{2+} inhibited contraction much more effectively, suggests 5-HT activates Ca_L and other Ca^{2+} influx pathways, including NSCCs, in vessels from normoxic and LTH sheep.

To begin to assess pharmacologically the role of NSCC during 5-HT-induced contractility, we exposed sheep pulmonary arteries to 50 μM SKF 96365 (SKF) in the presence of 10 μM nifedipine. We used these two drugs in combination because SKF can inhibit Ca_L in addition to blocking a number of transient receptor potential (TRP) channel isoforms (TRPC1, 3, and 6) that encode for nonselective cation channels (Krautwurst et al., 1994; Wang et al., 2004). Figure 4 also shows the influence of SKF and nifedipine on the average relative contraction in vessels from normoxic (11 ± 3%; $n = 14/N = 15$) compared to LTH (22 ± 5%; $n = 12/N = 14$) sheep. This drug combination reduced contraction equally in vessels from normoxic and LTH animals, and was just as effective as Ca^{2+} removal, 10 mM Ni^{2+}, or 10 μM verapamil.

The additive effects of SKF and nifedipine on the inhibition of 5-HT-induced pulmonary artery contraction led to additional experiments. These studies were designed to discrimi-

nate pharmacologically the various canonical TRP channels (TRPC) inhibited by SKF as well as melastatin TRP channels (TRPM) and sodium–calcium exchangers (NCX) that are likely important to 5-HT elicited contraction and affected by long-term hypoxia. This pharmacological profiling was performed with a series of inorganic and organic blockers that target TRPC, TRPM, and NCX with varying efficacy.

Figure 5 shows average arterial contractions normalized to an initial 10 μM 5-HT-induced contraction, in the presence and absence of 500 μM Ni^{2+}, 100 μM Gd^{3+}, and 100 μM La^{3+}. These metals were chosen because nickel in submillimolar concentrations, and lanthanides are well-described NSCC and TRP channel inhibitors (Ramsey et al., 2006; Wilson et al., 2005). Within the normoxic group, Ni^{2+} (77 ± 6%; $n = 11/N = 3$), Gd^{3+} (54 ± 6%; $n = 8/N = 3$) and La^{3+} (63 ± 11%; $n = 9/N = 3$) significantly reduced contraction compared to control (110 ± 6; $n = 14/N = 5$). These findings were similar in vessels from LTH sheep, where Ni^{2+} (72 ± 3%; $n = 9/N = 3$), Gd^{3+} (54 ± 5%; $n = 9/N = 3$) and La^{3+} (59 ± 8%; $n = 9/N = 3$) also significantly reduced arterial tension compared to control (106 ± 5; $n = 12/N = 3$).

Figure 6 shows averages of the normalized arterial recordings to 10 μM 5-HT in the presence and absence of organic blockers in vessels from normoxic and LTH animals. The organic compounds and their dosages were chosen for their actions and overlapping pharmacology on various isoforms of TRPC and TRPM, as well as NCX, which may be important during 5-HT-elicited contraction and many of which are inhibited by SKF 96365. 2-APB was chosen because it blocks TRPC1, 5, 6, and TRPM3, 8 and STIM-ORAI channels in the 50–100 μM range, although it can also activate channels (Goto et al., 2010; Ramsey et al., 2006; Wang et al., 2009). Flufenamic acid also blocks TRPC3, 5, and 7, as well as TRPM2, 4, and 5, but may activate TRPC6 (Ramsey et al., 2006). Spermine at 100 μM preferentially blocks TRPM4, 5, and 7 (Ramsey et al., 2006). KBR at 30 μM blocks TRPC3, 5, and 6, as well as NCX1, 2, 3 (Kraft, 2007), while the same concentration of SN-6 is only

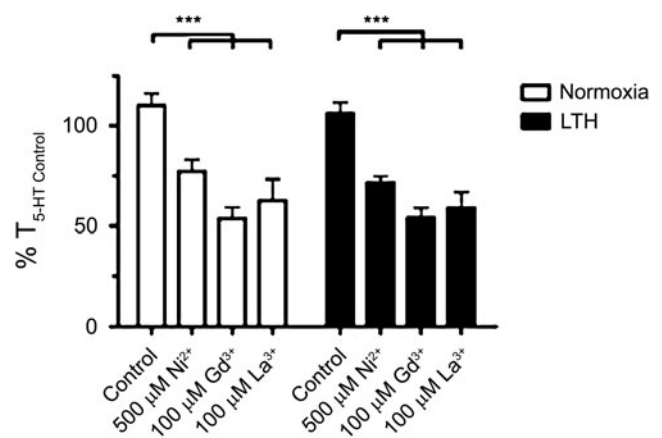**FIG. 5.** Gd^{3+}, La^{3+}, and low dose Ni^{2+} inhibit 5-HT-elicited pulmonary arterial ring contractility in sheep. *Bars* indicate mean ± S.E.M. based on isometric tension recordings of pulmonary arterial rings from adult sheep constricted with 10 μM 5-HT in the absence or presence of 500 μM Ni^{2+}, 100 μM Gd^{3+}, or 100 μM La^{3+} in normoxic (*open*) or LTH (*solid*) sheep. Values of the 5-HT-induced contraction are expressed as % T5-HT Control for the noted condition. ***$p < 0.001$ denotes significant difference by 2-way ANOVA.
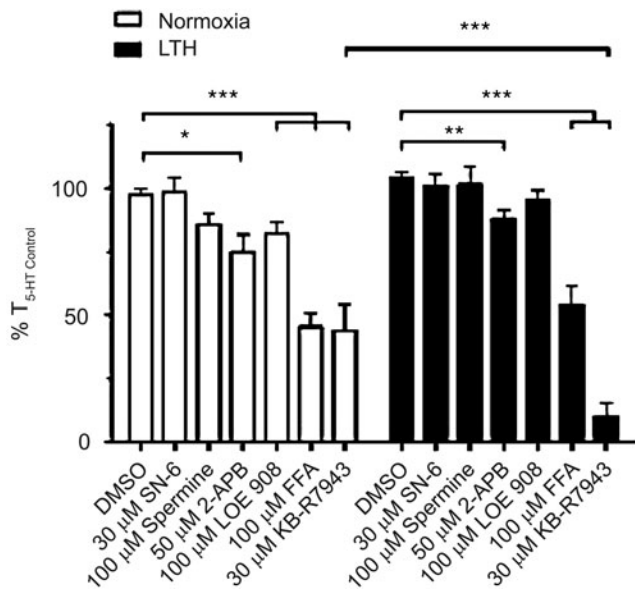
FIG. 6. Summary of the effect of organic NSCC and NCX antagonists on 5-HT-elicited pulmonary artery constriction. *Bars* indicate mean±S.E.M. of 5-HT-induced contraction expressed as a % of the initial $10\,\mu M$ 5-HT stimulation (% T5-HT Control) for the noted condition in pulmonary arterial rings from normoxic (*open*) or LTH (*solid*) sheep. *$p < 0.05$, **$p < 0.01$, ***$p < 0.001$) denotes significant difference by 2-way ANOVA.

known to block NCX1, 2, 3 (Kita and Iwamoto, 2007). LOE was chosen because it is a putative inhibitor of native NSCC activated by arginine vasopressin but not store depletion in A7R5 myocytes (Krautwurst et al., 1994).

Figure 6 shows that in normoxic sheep neither SN-6 (98 ± 6; $n = 11/N = 4$) nor spermine (86 ± 5; $n = 13/N = 5$) reduced contraction, as compared to control (97 ± 3; $n = 45/N = 14$). 2-APB (75 ± 7; $n = 16/N = 5$) and LOE (82 ± 5; $n = 14/N = 3$) modestly reduced tension, while FFA (46 ± 6; $n = 13/N = 5$) and KBR (44 ± 10; $n = 11/N = 4$) substantially reduced tension, as compared to control. In LTH sheep the profiling was similar, SN-6 (101 ± 5; $n = 9/N = 3$), spermine (101 ± 7; $n = 9/N = 3$), and LOE (95 ± 4; $n = 9/N = 3$) did not significantly reduce the 5-HT- elicited tension, as compared to control (104 ± 3; $n = 21/N = 7$). 2-APB (88 ± 4; $n = 18/N = 5$) modestly reduced tension, while FFA (54 ± 7; $n = 8/N = 3$) and KBR (10 ± 5; $n = 9/N = 3$) significantly depressed 5-HT-mediated contraction compared to control. Interestingly, only KBR inhibited contraction to a greater extent in arteries from LTH compared to normoxic sheep.

To assess further the influence of LTH on vascular reactivity, we performed a series of laser scanning confocal microscopy studies. In these experiments, cytosolic Ca^{2+} was monitored in myocytes using *in-situ* approaches, in the absence as well as presence of $10\,\mu M$ 5-HT. These studies were performed because we previously showed that cytosolic Ca^{2+} oscillations are critical to serotonin-mediated pulmonary arterial contraction (Wilson et al., 2005). Figures 7A (normoxic) and 7C (LTH) show confocal micrographs of the Fluo-4 signal from regions of interest in pulmonary arterial rings of adult sheep at the time points shown by the arrows in normoxic (Fig. 7B) and LTH (Fig. 7D) for their respective time series traces. Each region of interest, numbered 1 through 4 (Figs. 7A

and 7C), corresponds to an individual myocyte in the arterial wall. Region 5 is a ~ 33 X $33\,\mu m$ box ($1\,mm^2$) and is representative of the area used to measure the number of responsive cells in live preparations and to count the number of smooth muscle nuclei in fixed preparations. Figures 7B (normoxic) and 7D (LTH) show the Ca^{2+}-signaling behavior of four individual myocytes (regions 1–4, Figs. 7A and 7C) expressed as the average baseline-subtracted fractional fluorescence intensity tracing (F/Fo) over time. The cell to cell variability in frequency and fluorescence-amplitude indicate the complexity of the $Ca2+$ signaling events. Notably, this complexity is important to arterial contraction (Perez and Sanderson, 2005; Wilson et al., 2005). Figures 7E and 7F provide averaged data, based on analysis of the above-mentioned regions of interest. Figure 7E shows that the number of basal and stimulated myocytes in each mm^2 of the pulmonary arterial wall is unaltered by LTH, although 5-HT dramatically increased the number of cells with cytosolic Ca^{2+} oscillations. Figure 7F shows that, although 5-HT increased the myocyte firing frequency, neither basal nor 5-HT-stimulated firing rates were affected by LTH.

Structural studies were then performed in arteries of the same branch orders and similar diameter as those used for the functional studies. In these experiments, measurements of the smooth muscle and adventitial layers were made using confocal imaging approaches of fluorescently-labeled arteries. Figures 8A and 8B show representative confocal microscopy images of arteries from normoxic and LTH sheep, respectively. These figures show that the smooth muscle cells and their nuclei are elongated, and that the cells of these samples are indistinguishable. Figures 8C–8E show the thickness of the smooth muscle layer, total wall thickness, and the ratio of these two measurements. Figure 8C shows that the thickness of the alpha-smooth muscle layers were similar in vessels from sheep exposed to normoxia or LTH, being $5.4 \pm 0.9\,\mu m$ ($N = 7$ arteries) and $4.8 \pm 0.4\,\mu m$ ($N = 10$ arteries), respectively. Figure 8D shows that the thicknesses of the arterial walls in these vessels were also similar, being $16.3 \pm 0.9\,\mu m$ and $16.7 \pm 0.5\,\mu m$, respectively. Figure 8E shows that the ratio of the alpha-smooth muscle layer to the total thickness of the arterial wall was unchanged. Overall, these studies show that LTH did not cause structural remodeling in these arteries.

Discussion

The present study is the first examination of serotonergic-induced contraction in pulmonary arteries from high-altitude acclimatized adult sheep. Our results indicate that arterial structure, as well as high K^+- and 5-HT-induced pulmonary vascular contractility, were preserved during LTH. Moreover, $5\text{-}HT_{2A}$ receptor function, which is the most important receptor to 5-HT-elicited contractility in pulmonary arteries from sheep, also was maintained following LTH. Extracellular Ca^{2+} influx through NSCC and Ca_L channels was integral to serotonergic-dependent pulmonary artery contraction and maintained after prolonged high altitude living.

The lack of a substantial change in 5-HT-elicited pulmonary vascular contraction by LTH is an important finding because it suggests that pulmonary arterial contraction in sheep is more resilient to low oxygen tensions as compared to other species. In particular, 5-HT-elicited pulmonary arterial contraction was significantly increased by LTH in adult rats (MacLean et al., 1996). The maintenance of 5-HT contraction
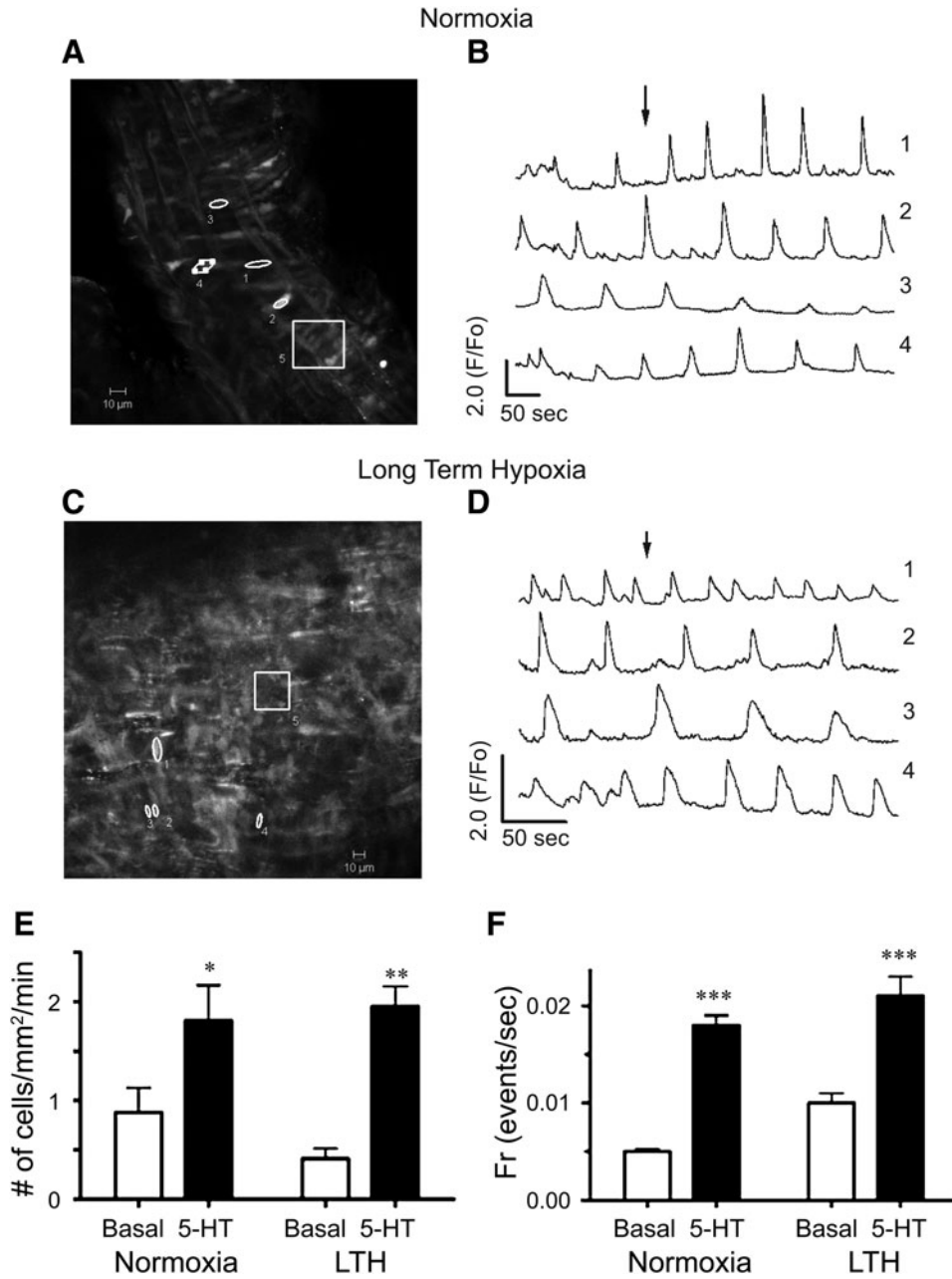
Normoxia

A

B

Long Term Hypoxia

C

D

E

F

FIG. 7. Effect of 10 μM 5-HT on spatial and temporal Ca^{2+} signaling characteristics recorded *in situ*. Micrographs of the Fluo-4 fluorescence in pulmonary arterial myocytes from **(A)** normoxic and **(C)** LTH sheep. Regions 1 to 4 indicate individual pulmonary arterial myocytes, and region 5 represents a 1 mm^2 area used to calculate the number of responsive cells in each arterial segment. Average baseline-subtracted fractional fluorescence (F/Fo) traces are shown for regions 1–4 for pulmonary arteries from **(B)** normoxic and **(D)** LTH sheep. *Arrows* in panels **B** and **D** indicate the time corresponding to the associated fluorescence micrographs shown in panels **A** and **C**. **(E)** *Bars* indicate mean $\pm$ S.E.M. number of myocytes with Ca^{2+} responses each minute in a 1 mm^2 area in the absence (*open*) and presence (*solid*) of 10 μM 5-HT. **(F)** *Bars* indicate mean $\pm$ S.E.M. frequency of Ca^{2+} events in the absence (*open*) and presence (*solid*) of 10 μM 5-HT. *$p < 0.05$, **$p < 0.01$, or ***$p < 0.001$ denotes significant difference from control based on 2-way ANOVA. Images were made with a 40X c-Apochromat water immersion objective.

in adult sheep may provide a protective effect, as compared to enhanced reactions in rats, because it limits the influence of an already vasoreactive environment (LTH) and tempers extreme, and possibly deleterious, vascular responses to 5-HT.

The comparable pulmonary arterial vasoreactivity to 5-HT in vessels from normoxic and LTH sheep may be explained partially by differential 5-HT receptor function compared to

rodents. Several studies indicate that 5-HT1B/D is important in the development of pulmonary hypertension in rats and mice (Keegan et al., 2001; MacLean et al., 2000). Previous studies also show that pharmacological synergism between 5-HT$_{1B/D}$ and 5-HT$_{2A}$ receptors heighten 5-HT-mediated vasoconstriction in LTH rats (Keegan et al., 2001). In comparison, LTH did not greatly influence the relative roles of 5HT$_{1B/D}$
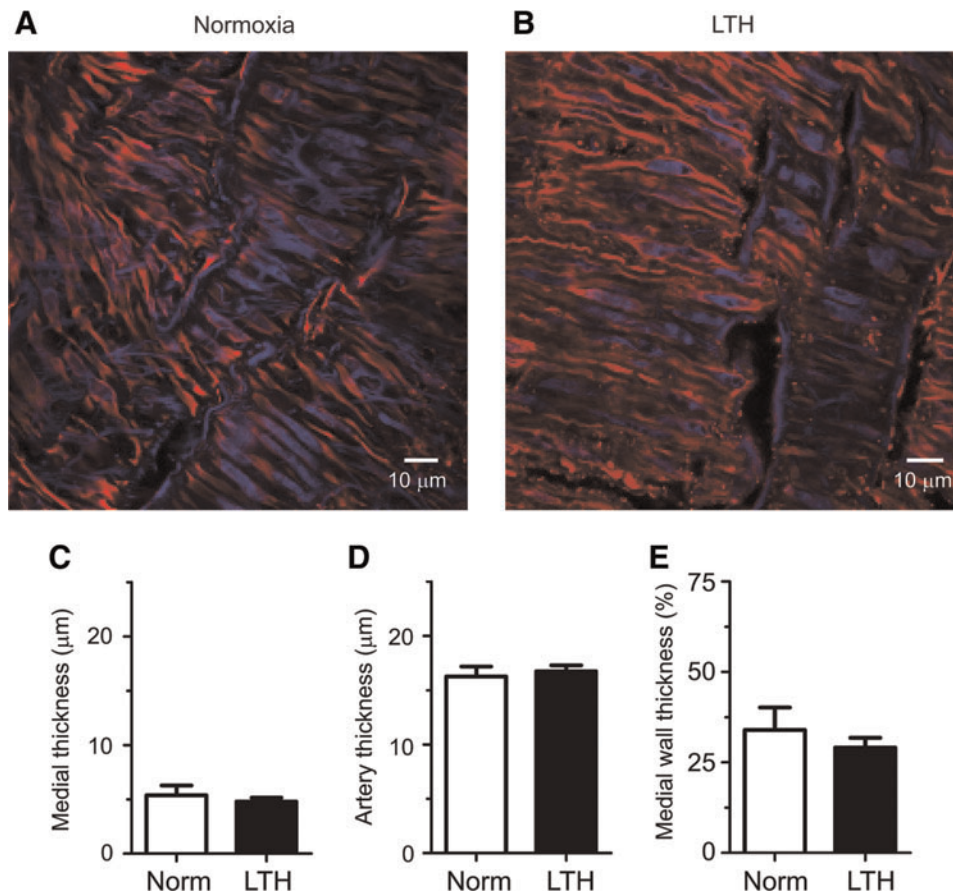
FIG. 8. LTH fails to increase the medial wall thickness in pulmonary arteries from adult sheep. Representative confocal micrographs from **(A)** normoxic and **(B)** LTH sheep arteries. Thickness of **(C)** anti-alpha-smooth muscle actin layer and **(D)** total arterial wall (in μm) and their ratio **(E)** (expressed as a percentage). *Bars* indicate mean±S.E.M. Images and measurements were made optically using a 63X Apochromat oil immersion objective and confocal laser scanning microscopy approaches in multiple sites in each artery.

to 5-HT$_{2A}$ receptors in the present studies. This lack of enhancement of 5-HT$_{1B/D}$ receptor-mediated contraction could be a biomarker that sheep are relatively protected, and are less prone to hypoxia-related pulmonary hypertension.

The finding that extracellular Ca^{2+} entry is important to 5-HT-dependent pulmonary artery contraction in sheep was not surprising, and builds on our previous studies in pulmonary arterial myocytes from dogs and sheep (Goyal et al., 2008; Wilson et al., 2005). However, the findings that Ca^{2+} signals and Ca^{2+}-dependent contraction are preserved following LTH, contrasts studies in rats where LTH depressed ET-1, angiotensin II, and ATP-dependent cytosolic Ca^{2+} signaling of pulmonary arterial myocytes (Bonnet et al., 2001; Shimoda et al., 2000). This provides additional evidence that adult sheep resist deleterious effects of high-altitude living on serotonin-mediated Ca^{2+} signaling in pulmonary arterial myocytes.

We find that 5-HT-dependent pulmonary arterial contraction in sheep is dependent on Ca^{2+} influx through both voltage-sensitive and -insensitive pathways. Experimentally, nifedipine and diltiazem each reduced contraction by about one-quarter. Among the Ca_L antagonists tested, only nifedipine was less effective in vessels from LTH animals. This finding is similar to the reduced role for Ca_L during ET-1 stimulation of pulmonary arterial myocytes in LTH rats

(Shimoda et al., 2000). However, because diltiazem reduced 5-HT-dependent contraction in pulmonary arteries from normoxic and LTH sheep to a similar extent, it is unlikely that LTH alters Ca_L expression. In comparison to the modest reduction in contraction due to Ca_L inhibition with nifedipine or diltiazem, blocking Ca^{2+} entry with millimolar Ni^{2+}, KBR, the combination of SKF and nifedipine, verapamil, or by removing extracellular Ca^{2+}, reduced 5-HT-elicited contraction more effectively. Together, these data indicate that voltage-independent Ca^{2+} entry is more vital to serotonin-mediated pulmonary vascular reactivity than voltage-dependent pathways.

The substantial block of contraction by verapamil, relative to diltiazem and nifedipine, was unexpected because verapamil primarily blocks Ca_L. However, verapamil can inhibit TRPC3 channels cloned from humans (Ramsey et al., 2006; Zhu et al., 1998). This finding suggests that TRPC3 serves an important role to 5-HT-mediated contraction in sheep pulmonary arteries. This builds on molecular evidence showing that TRPC3 is important to receptor-coupled cerebral arterial contraction (Adebiyi et al., 2010; Reading et al., 2005). The reduction in contraction by inorganic blockers of Ca^{2+} entry also provides details regarding the importance of various TRP channels to 5-HT-dependent pulmonary arterial contraction in sheep. Although the low-concentrations of Ni^{2+}, Gd^{3+}, and

La^{3+} that were used in the present studies cannot be used to fully discriminate the TRP channel isoforms involved, each one reduced 5-HT-elicited contraction by roughly one-third. It is not surprising that TRP channels are likely important to voltage-independent Ca^{2+} influx and contraction in *ovine* pulmonary arteries, as they contribute significantly in other species (Lin et al., 2004; Wang et al., 2004; Yang et al., 2006).

The varied inhibition of contraction by the organic blockers of NSCC used in the present studies provides more details concerning the importance of TRP channels to serotonin-dependent contraction. The marked inhibition of contraction by KBR, SKF, and verapamil, modest inhibition by FFA and 2-APB, and lack of an effect of spermine, substantiate that one or more TRPC or TRPM channels are activated by 5-HT. Based on this pharmacological profile, the influence of verapamil, and the expression of TRP gene products in pulmonary arterial myocytes of mice, rats, dogs, and fetal sheep, the most likely candidates include: TRPC3, TRPC5, TRPC6, and possibly STIM-ORAI (Lin et al., 2004; Lu et al., 2008; Resnik et al., 2007; Walker et al., 2001; Yang et al., 2006). The augmented inhibitory action of KBR to sheep pulmonary arterial reactivity after acclimatization to high altitude suggests that TRPC3, TRPC5, or TRPC6 expression may be increased. The finding also is important because LTH increases TRPC1 and TRPC6 expression in rats (Lin et al., 2004), and TRPC6 expression is coupled to proliferation of rat pulmonary arterial myocytes (Yu et al., 2003) and those from patients with idiopathic pulmonary hypertension (Yu et al., 2004). The expression of TRP genes in adult sheep pulmonary arterial myocytes, and the potential changes due to LTH, remains to be determined. However, the functional comparisons suggest that increases in the expression of TRP gene(s) inhibited by KBR represent acclimatization responses to high altitude. The ramifications of this increase in KBR sensitivity are presently unknown, but could be an early adaptive response to high altitude.

The finding that SN-6 did not block pulmonary arterial contraction suggests that the KBR inhibition is not mediated by reverse-mode NCX activity in sheep pulmonary arteries. This differs from human pulmonary arterial myocytes in which reverse-mode Na^+–Ca^{2+} exchange is important, and accentuated in myocytes from idiopathic pulmonary hypertension patients (Zhang et al., 2007). The lack of an effect of SN-6 provides further support that voltage-insensitive pathways, and specifically TRP channels, are critical to pulmonary arterial contraction in sheep (Kraft, 2007; Ramsey et al., 2006).

Of note, our study did not examine the possible role of the serotonin transporter (5-HTT) in pulmonary vasoconstriction. There is published evidence that 5-HT induces pulmonary artery smooth muscle cell and arterial fibroblast proliferation through the activity of the 5-HTT (Lee et al., 1994), as well as $5-HT_{2A}$ (Welsh et al., 2004). There is also limited evidence that 5-HTT can modulate pulmonary vascular contraction through cooperation with $5-HT_{1B}$ (Lawrie et al., 2005; Morecroft et al., 2005). However, the process of 5-HT-induced pulmonary artery contraction mediated through 5-HTT has not been as clearly delineated as the role for 5-HT receptors (Keegan et al., 2001; MacLean et al., 2000; Wilson et al., 2005). Therefore, although 5-HTT may be significant to pulmonary vascular remodeling and the pathophysiology of pulmonary hypertension, the importance of 5-HTT to ovine pulmonary vasoconstriction and the influence of high altitude exposure on their function remains to be determined.

LTH due to living at high altitude can cause remodeling of the pulmonary vasculature in some species. Thickening of the smooth muscle layer as well as adventitia are observed in pulmonary arteries in animal models and humans who have pulmonary hypertension (Stenmark et al., 2009; Tucker et al., 1975). Still, the pulmonary arteries from our adult sheep that resided at ~13,000 feet for over 3 months did not have structural changes indicative of the development of pulmonary hypertension. This compares with newborn sheep that underwent gestation with birth at high altitude that develop pulmonary hypertension (Herrera et al., 2007; Herrera et al., 2010). Moreover, distal but not proximal arteries of term fetal sheep that underwent gestation at high altitude had medial wall thickening consistent with the development of pulmonary hypertension (Bixby et al., 2007; Xue et al., 2008). This suggests that gestational LTH increases the predisposition for the development of pulmonary hypertension in fetal sheep, whereas adults of this model appear more resistant to structural and functional deficits induced by LTH.

In summary, our experiments indicate that adult sheep acclimatize well to LTH. These sheep appear to be protected from thickening of smaller arteries and LTH-induced pulmonary artery hyper-reactivity, at least with respect to 5-HT and KCl. Extracellular Ca^{2+} influx through a combination of Ca_L and TRP channels is critical to 5-HT contraction. In comparison to studies performed in rats, the data suggest that the maintenance of $5HT_{1B/D}$ receptor and Ca_L function are important responses that restrict pulmonary vascular hyper-responsiveness in the hypoxic setting.

Acknowledgments

Author Disclosure Statement

No competing financial interests exist.

References

Adebiyi A, Zhao G, Narayanan D, Thomas-Gatewood CM, Bannister JP, and Jaggar JH. (2010). Isoform-selective physical coupling of TRPC3 channels to IP3 receptors in smooth muscle cells regulates arterial contractility. Circ Res 106:1603–1612.

Bixby CE, Ibe BO, Abdallah MF, Zhou W, Hislop AA, Longo LD, and Raj JU. (2007). Role of platelet-activating factor in pulmonary vascular remodeling associated with chronic high altitude hypoxia in ovine fetal lambs. Am J Physiol Lung Cell Mol Physiol 293:L1475–L1482.

Bonnet S, Belus A, Hyvelin JM, Roux E, Marthan R, and Savineau JP. (2001). Effect of chronic hypoxia on agonist-induced tone and calcium signaling in rat pulmonary artery. Am J Physiol Lung Cell Mol Physiol 281:L193–L201.

Goto J-I, Suzuki AZ, Ozaki S, Matsumoto N, Nakamura T, Ebisui E, Fleig A, Penner R, and Mikoshiba K. (2010). Two novel 2-aminoethyl diphenylborinate (2-APB) analogues differentially activate and inhibit store-operated Ca^{2+} entry via STIM proteins. Cell Calcium 47:1–10.

Goyal R, Creel KD, Chavis E, Smith GD, Longo LD, and Wilson SM. (2008). Maturation of intracellular calcium homeostasis in sheep pulmonary arterial smooth muscle cells. Am J Physiol Lung Cell Mol Physiol 295:L905–914.

Heffner JE, Sahn SA, and Repine JE. (1987). The role of platelets in the adult respiratory distress syndrome. Culprits or bystanders? Am Rev Respir Dis 135:482–492.

Herrera EA, Pulgar VM, Riquelme RA, Sanhueza EM, Reyes RV, Ebensperger G, Parer JT, Valdez EA, Giussani DA, Blanco CE, Hanson MA, and Llanos AJ. (2007). High-altitude chronic hypoxia during gestation and after birth modifies cardiovascular responses in newborn sheep. Am J Physiol Regul Integr Comp Physiol 292:R2234–2240.

Herrera EA, Riquelme RA, Ebensperger G, Reyes RV, Ulloa CE, Cabello G, Krause BJ, Parer JT, Giussani DA, and Llanos AJ. (2010). Long-term exposure to high-altitude chronic hypoxia during gestation induces neonatal pulmonary hypertension at sea level. Am J Physiol Regul Integr Comp Physiol 299:R1676–R1684.

Hinton JM, Hill P, Jeremy J, and Garland C. (2000). Signalling pathways activated by 5-HT(1B)/5-HT(1D) receptors in native smooth muscle and primary cultures of rabbit renal artery smooth muscle cells. J Vasc Res 37:457–468.

Hirenallur SD, Haworth ST, Leming JT, Chang J, Hernandez G, Gordon JB, and Rusch NJ. (2008). Upregulation of vascular calcium channels in neonatal piglets with hypoxia-induced pulmonary hypertension. Am J Physiol Lung Cell Mol Physiol 295:L915–924.

Hobai IA, Bates JA, Howarth FC, and Levi AJ. (1997). Inhibition by external Cd^{2+} of Na/Ca exchange and L-type Ca channel in rabbit ventricular myocytes. Am J Physiol Renal Physiol 272:H2164–H2172.

Hollywood MA, Woolsey S, Walsh IK, Keane PF, McHale NG, and Thornbury KD. (2003). T- and L-type Ca^{2+} currents in freshly dispersed smooth muscle cells from the human proximal urethra. J Physiol 550:753–764.

Kamitomo M, Longo LD, and Gilbert RD. (1994). Cardiac function in fetal sheep during two weeks of hypoxemia. Am J Physiol Renal Physiol 266:R1778–R1785.

Keegan A, Morecroft I, Smillie D, Hicks MN, and MacLean MR. (2001). Contribution of the 5-HT1B receptor to hypoxia-induced pulmonary hypertension: Converging evidence using 5-HT1B-receptor knockout mice and the 5-HT1B/1D-receptor antagonist GR127935. Circ Res 89:1231–1239.

Kita S and Iwamoto T. (2007). Inhibitory mechanism of SN-6, a novel benzyloxyphenyl Na^+/Ca^{2+} exchange inhibitor. Ann NY Acad Sci 1099:529–533.

Kraft R. (2007). The Na^+/Ca^{2+} exchange inhibitor KB-R7943 potently blocks TRPC channels. Biochem Biophys Res Commun 361:230–236.

Krautwurst D, Degtiar VE, Schultz G, and Hescheler J. (1994). The isoquinoline derivative LOE 908 selectively blocks vasopressin-activated nonselective cation currents in A7r5 aortic smooth muscle cells. Naunyn Schmiedebergs Arch Pharmacol 349:301–307.

Lauweryns JM, de Bock V, Guelinckx P, and Decramer M. (1983). Effects of unilateral hypoxia on neuroepithelial bodies in rabbit lungs. J Appl Physiol 55:1665–1668.

Lawrie A, Spiekerkoetter E, Martinez EC, Ambartsumian N, Sheward WJ, MacLean MR, Harmar AJ, Schmidt AM, Luka-nidin E, and Rabinovitch M. (2005). Interdependent serotonin transporter and receptor pathways regulate S100A4/Mts1, a gene associated with pulmonary vascular disease. Circ Res 97:227–235.

Lee SL, Wang WW, Lanzillo JJ, and Fanburg BL. (1994). Serotonin produces both hyperplasia and hypertrophy of bovine pulmonary artery smooth muscle cells in culture. Am J Physiol Renal Physiol 266:L46–L52.

Lin MJ, Leung GP, Zhang WM, Yang XR, Yip KP, Tse CM, and Sham JS. (2004). Chronic hypoxia-induced upregulation of store-operated and receptor-operated Ca^{2+} channels in pulmonary arterial smooth muscle cells: A novel mechanism of hypoxic pulmonary hypertension. Circ Res 95:496–505.

Longo LD, Ueno N, Zhao Y, Zhang L, and Pearce WJ. (1996). NE-induced contraction, alpha 1-adrenergic receptors, and Ins(1,4,5)P3 responses in cerebral arteries. Am J Physiol Renal Physiol 270:H91–H923.

Lu W, Wang J, Shimoda LA, and Sylvester JT. (2008). Differences in STIM1 and TRPC expression in proximal and distal pulmonary arterial smooth muscle are associated with differences in Ca^{2+} responses to hypoxia. Am J Physiol Lung Cell Mol Physiol 295:L104–113.

MacLean MR, Herve P, Eddahibi S, and Adnot S. (2000). 5-hydroxytryptamine and the pulmonary circulation: Receptors, transporters and relevance to pulmonary arterial hypertension. Br J Pharmacol 131:161–168.

MacLean MR, Sweeney G, Baird M, McCulloch KM, Houslay M, and Morecroft I. (1996). 5-Hydroxytryptamine receptors mediating vasoconstriction in pulmonary arteries from control and pulmonary hypertensive rats. Br J Pharmacol 119:917–930.

Morecroft I, Loughlin L, Nilsen M, Colston J, Dempsie Y, Sheward J, Harmar A, and MacLean MR. (2005). Functional Interactions between 5-hydroxytryptamine receptors and the serotonin transporter in pulmonary arteries. J Pharmacol Exper Therapeut 313:539–548.

Ng LC, Wilson SM, McAllister CE, and Hume JR. (2007). Role of InsP3 and ryanodine receptors in the activation of capacitative Ca^{2+} entry by store depletion or hypoxia in canine pulmonary arterial smooth muscle cells. Br J Pharmacol 152:101–111.

Penaloza D and Arias-Stella J. (2007). The heart and pulmonary circulation at high altitudes: Healthy highlanders and chronic mountain sickness. Circulation 115:1132–1146.

Perez JF and Sanderson MJ. (2005). The contraction of smooth muscle cells of intrapulmonary arterioles is determined by the frequency of Ca^{2+} oscillations induced by 5-HT and KCl. J Gen Physiol 125:555–567.

Ramsey IS, Delling M, and Clapham DE. (2006). An introduction to TRP channels. Ann Rev Physiol 68:619–647.

Reading SA, Earley S, Waldron BJ, Welsh DG, and Brayden JE. (2005). TRPC3 mediates pyrimidine receptor-induced depolarization of cerebral arteries. Am.J.Physiol Heart Circ.Physiol 288:H2055–H2061.

Resnik ER, Keck M, Sukovich DJ, Herron JM, and Cornfield DN. (2007). Chronic intrauterine pulmonary hypertension increases capacitative calcium entry in fetal pulmonary artery smooth muscle cells. Am J Physiol Lung Cell Mol Physiol 292:L953–959.

Shimoda LA, Sham JS, Shimoda TH, and Sylvester JT. (2000). L-type Ca^{2+} channels, resting $[Ca(2+)](i)$, and ET-1-induced responses in chronically hypoxic pulmonary myocytes. Am J Physiol Lung Cell Mol Physiol 279:L884–L894.

Stenmark KR, Meyrick B, Galie N, Mooi WJ, and McMurtry IF. (2009). Animal models of pulmonary arterial hypertension: The hope for etiological discovery and pharmacological cure. Am J Physiol Lung Cell Mol Physiol 297:L1013–1032.

Toga H, Ibe BO, and Raj JU. (1992). *In vitro* responses of ovine intrapulmonary arteries and veins to endothelin-1. Am J Physiol Renal Physiol 263:L15–L21.

Tucker A, McMurtry IF, Reeves JT, Alexander AF, Will DH, and Grover RF. (1975). Lung vascular smooth muscle as a determinant of pulmonary hypertension at high altitude. Am J Physiol 228:762–767.

Voelkel NF and Tuder RM. (1995). Cellular and molecular mechanisms in the pathogenesis of severe pulmonary hypertension. Eur Respir J 8:2129–2138.

Walker RL, Hume JR, and Horowitz B. (2001). Differential expression and alternative splicing of TRP channel genes in smooth muscles. AJP Cell Physiology 280:C1184–C1192.

Wang J, Shimoda LA, and Sylvester JT. (2004). Capacitative calcium entry and TRPC channel proteins are expressed in rat distal pulmonary arterial smooth muscle. Am J Physiol Lung Cell Mol Physiol 286:L848–L858.

Wang Y, Deng X, Zhou Y, Hendron E, Mancarella S, Ritchie MF, Tang XD, Baba Y, Kurosaki T, Mori Y, Soboloff J, and Gill DL. (2009). STIM protein coupling in the activation of Orai channels. Proc Natl Acad Sci USA 106:7391-7396.

Ward JP and Snetkov VA. (2004). Determination of signaling pathways responsible for hypoxic pulmonary vasoconstriction: Use of the small vessel myograph. Methods Enzymol 381:71–87.

Welsh DJ, Harnett M, MacLean M, and Peacock AJ. (2004). Proliferation and signaling in fibroblasts: Role of 5-hydroxytryptamine$_{2A}$ receptor and transporter. Am J Respir Crit Care Med 170:252–259.

Wilson SM, Mason HS, Ng LC, Montague S, Johnston L, Nicholson N, Mansfield S, and Hume JR. (2005). Role of basal extracellular Ca^{2+} entry during 5-HT-induced vasoconstriction of canine pulmonary arteries. Br J Pharmacol 144:252–264.

Xue Q, Ducsay CA, Longo LD, and Zhang L. (2008). Effect of long-term high-altitude hypoxia on fetal pulmonary vascular contractility. J Appl Physiol 104:1786–1792.

Yang XR, Lin MJ, McIntosh LS, and Sham JS. (2006). Functional expression of transient receptor potential melastatin- and vanilloid-related channels in pulmonary arterial and aortic smooth muscle. Am J Physiol Lung Cell Mol Physiol 290: L1267–L1276.

Yu Y, Fantozzi I, Remillard CV, Landsberg JW, Kunichika N, Platoshyn O, Tigno DD, Thistlethwaite PA, Rubin LJ, and Yuan JX. (2004). Enhanced expression of transient receptor potential channels in idiopathic pulmonary arterial hypertension. Proc Natl Acad Sci USA 101:13861–13866.

Yu Y, Sweeney M, Zhang S, Platoshyn O, Landsberg J, Rothman A, and Yuan JX. (2003). PDGF stimulates pulmonary vascular smooth muscle cell proliferation by upregulating TRPC6 expression. Am J Physiol Cell Physiol 284:C316–C330.

Zhang S, Dong H, Rubin LJ, and Yuan JX. (2007). Upregulation of Na^+/Ca^{2+} exchanger contributes to the enhanced Ca^{2+} entry in pulmonary artery smooth muscle cells from patients with idiopathic pulmonary arterial hypertension. Am J Physiol Cell Physiol 292:C2297–C2305.

Zhu X, Jiang M, and Birnbaumer L. (1998). Receptor-activated Ca^{2+} influx via human Trp3 stably expressed in human embryonic kidney (HEK)293 cells. Evidence for a non-capacitative Ca2+ entry. J Biol Chem 273:133–142.

Address correspondence to:
Sean M Wilson, Ph.D.
Center for Perinatal Biology
Loma Linda University School of Medicine
11234 Anderson Street
Loma Linda CA, 92350

E-mail: seanwilson@llu.edu